IEEE Photonics Journal
An IEEE Photonics Society Publication

Fiber-Optic Pressure Sensor Based on Tunable Liquid Crystal Technology

Volume 2, Number 3, June 2010

Jing Feng
Yun Zhao
Su-shan Li
Xiao-wen Lin
Fei Xu
Yan-qing Lu, Senior Member, IEEE

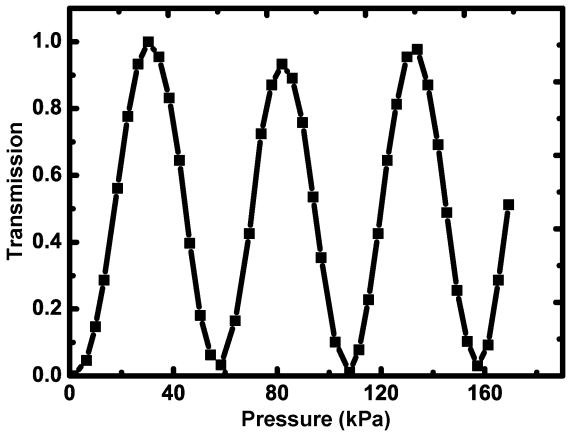

DOI: 10.1109/JPHOT.2010.2045365
1943-0655/$26.00 ©2010 IEEE

Fiber-Optic Pressure Sensor Based on Tunable Liquid Crystal Technology

Jing Feng, Yun Zhao, Su-shan Li, Xiao-wen Lin, Fei Xu, and Yan-qing Lu, *Senior Member, IEEE*

Department of Materials Science and Engineering and National Laboratory of Solid State Microstructures, Nanjing University, Nanjing 210093, China

DOI: 10.1109/JPHOT.2010.2045365

Manuscript received January 20, 2010; revised March 3, 2010. First published Online March 15, 2010. Current version published May 18, 2010. This work was supported in part by the 973/quantum manipulation program under Contract 2010CB327803 and Contract 2006CB921805 and in part by the National Natural Science Foundation of China program under Contract 10874080 and Contract 60977039. The authors acknowledge the support from the New Century Excellent Talents program and the Changjiang scholars program. Corresponding author: Y.-q. Lu (e-mail: yqlu@nju.edu.cn).

Abstract: We propose a photoelastic pressure sensor using a liquid crystal (LC) tunable fiber polarizer. The polarizer contains an etched single-mode fiber sealed in an LC cell. A low-index LC is used as a tunable birefringent cladding of the fiber. Any electric-field-induced LC director reorientation may thus affect the fiber's light-guiding characteristics. Different polarization states experience different LC cladding indices. The transmittance contrast between the x- and y-polarized modes reaches 31.9 dB, which is sensitive enough to monitor any polarization state change in the fiber. A pressure sensor with the sensitivity of 0.25 rad/N is thus demonstrated. The corresponding stress-optic coefficient of the fiber is measured at 1550-nm telecomm band. The advantages and applications of the LC tuning and sensing technologies are discussed.

Index Terms: Fiber-optic systems, sensors.

1. Background and Motivation

The past two decades have seen a rapidly growing interest in the field of fiber-optic sensors. In comparison with their electrical counterparts, fiber-optic sensors have many advantages, such as immunity to electromagnetic interference, miniature size, light weight, passive composition, high temperature, and multiplexing capability. As a result, fiber sensors have been developed for a variety of applications in industry, medicine, defense, and research to measure various physical parameters like pressure, temperature, acceleration, liquid level, voltage, and current. Moreover, the wide spread of optical fiber communication industry results in a substantial reduction in optical fiber sensor cost. It is even possible to integrate the fiber-optic sensing with communication functions to enable future applications in more advanced "smart grid" and "Internet of things" [1], [2].

On the other hand, liquid crystal (LC) has been successfully used in various fiber-optic communication devices, such as optical attenuators, optical switches, and polarization controllers with "tuning" capabilities [3]–[7]. In addition, LC is also reported in some pressure sensing devices, taking advantage of its deformation caused by pressure [8]–[11]. It would be very interesting to see if LC also works well in all-fiber sensors. More agile and low-loss sensing systems thus are expected.

In this paper, commercial communication grade optical fibers are used for pressure sensing through LC polarization control. A low-index LC acts as the cladding of a segment of etched fiber so that the transmission properties could be instantly manipulated by the external field. The field-induced

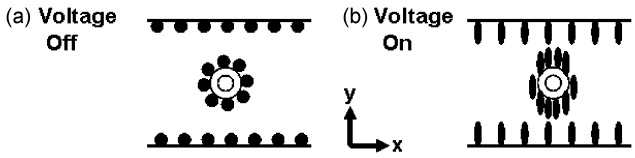

Fig. 1. Working principle of our fiber polarizer. (a) Voltage-off and (b) voltage-on situations.

LC director reorientation further affects the fiber's evanescent field. As different polarizations experience different LC cladding indices, a 31.9-dB transmittance contrast is achieved between two orthogonally polarized modes, which is high enough to monitor tiny photoelastic polarization changes in a fiber. A pressure sensor with the sensitivity of 0.25 rad/N is thus demonstrated. The corresponding stress-optic coefficient is obtained for silica optical fibers at the 1550-nm telecomm band. Other advantages and applications of our techniques are discussed.

2. Pressure Sensor and Fiber Polarizer

The photoelastic fiber-optic pressure sensor was first demonstrated by Spillman in 1982 [12]. Since the pressure sensing relies on detecting photoelastic polarization change, a high-contrast polarizer is required. Obviously, an all-fiber polarizer is much favorable for practical applications. Although various polarizer approaches have been proposed [13]–[15], they are all fixed. On the contrary, a LC fiber polarizer as shown in Fig. 1 might be more suitable for cascading or distributed pressure sensing in a reconfigurable sensing network.

As shown in Fig. 1, a segment of optical fiber is sandwiched between two Indium tin oxide (ITO) glass substrates with a spacing of 125 μm to form a tunable polarizer. The fiber is pre-etched nearly to its core so that the LC just acts as a cladding. In our experiment, a SMF-28 compatible fiber from Yangtze Corporation is employed. The etching length is $\sim$3 cm and the etched fiber diameter is easily adjustable by setting required etching time and temperature in hydrofluoric acid (HF).

To satisfy the light guiding condition, the fiber core should have a higher index than that of its cladding. Therefore, a low-index LC should be used. We select a nematic mixture LCMS-1550 from LCMS Ltd. Co., whose nematic range is from 16 °C to 77.3 °C. Its ordinary refractive index (n_o) is lower than the refractive index of fused silica fiber core $(n_{core} = 1.468)$, while the extraordinary refractive index (n_e) of LCMS-1550 is higher than the core index.

As we know, total internal reflection (TIR) enables light guiding in optical fibers. From Fig. 1(a), the LC molecules are originally homogeneously aligned along the fiber when there is no voltage applied. This is achieved by manually rubbing the LC cell substrates and the etched fiber axially with a rubbing cloth. Given that nematic LC molecules tend to lie parallel to the rubbing direction on a solid surface [16], the anchoring of the LC molecules is along the fiber in this situation. Both the input x- and y-polarized lights only see a LC cladding with n_o, lower than n_{core}, satisfying TIR. The light still could go through the fiber with no loss in an ideal case. However, an imperfect LC alignment may induce an insertion loss (IL), to some extent. On the other hand, the LC molecules would be realigned vertically in the cell as long as the driving voltage applied to the cell is high enough, which is shown in Fig. 1(b). For x-polarized light, it still experiences n_o, remaining guided. However, for y-polarized light, it now sees cladding index of n_e instead, which is larger than n_{core}. Therefore, the TIR condition is broken. Light cannot be localized in the fiber core, giving rise to attenuation. The transmittance contrast between x- and y- polarized light thus could be instantly controlled by an external field. A tunable fiber polarizer is obtained.

In our experiments, the fiber core dimension is 8.2 μm from its specification sheet. The etched area has the diameter of 18 μm, which means a thin 4.9-μm cladding remains. This actual case is a little more complicated than our quick analysis above. It is a doubly clad fiber with a thin original silica cladding and a surrounding LC cladding. When there is no voltage applied, it is still a single-mode fiber. However, the fundamental mode is split into two modes, i.e., HE_x and HE_y, with birefringent claddings [17]. When a driving voltage is applied to the LC cell, HE_x mode remains guided, while the HE_y mode leaks.

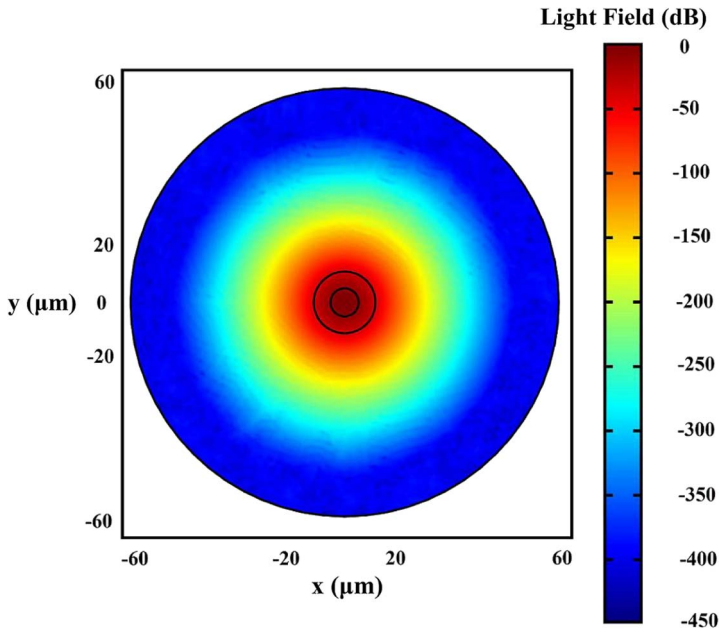

Fig. 2. Light field distribution of an LC cladding fiber simulated with COMSOL-Multiphysics.

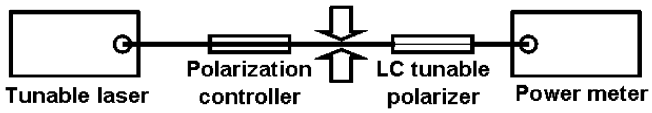

Fig. 3. Experimental setup to demonstrate the LC tunable fiber polarizer and pressure sensor.

To illustrate the light field distribution in a LC cladding fiber, Fig. 2 shows the COMSOL-Multiphysics (formerly FEMLAB, which is a finite element analysis software package) modeling results, corresponding to the voltage-off case. The central circle represents the fiber core, while the outer one corresponds to remaining cladding. $n_o = 1.449$ and $n_e = 1.50$ are used for the simulation. From the figure, the light field is well confined but there is still evident field outside the 18-μm etched fiber, which could be affected by the LC status. However, when a voltage is applied, the HE_x has no change, while HE_y can no longer be guided at the central core, which is equivalent to a polarizer along *x*-axis.

3. Experimental Results and Discussions

Fig. 3 depicts the schematic diagram of our experimental setup to characterize the LC-based fiber polarizer and demonstrate the pressure sensing. The 1550-nm light from a tunable laser (Santec TSL-210) is further controlled by an inline polarization controller to ensure a y-polarized light entering the LC tunable polarizer. The output light is measured by a fiber power meter (HP 8153A). As the LC cell is configured like an x-polarizer, the whole setup is like a typical cross-polarization interference filter. Any phase retardation induced in the fiber between the polarization controller and our LC cell can be detected according to the output power variation, which is the fundamental of our photoelastic pressure sensor.

Before the pressure measurement, the LC tunable fiber polarizer is characterized. When there is no voltage applied, the average IL is measured to be -1.4 dB, agreeing well with our prediction. The LC acts as a low-index cladding so that most light can be trapped and propagate in the fiber core. However, when a voltage is applied, y-polarized light portion is attenuated, and the LC cell makes an x-polarizer. The contrast ratio $(I_y : I_x)$ of the polarizer is tunable, as shown in Fig. 4. With the applied voltage increasing, the contrast becomes increasingly higher. It reaches -31.9 dB at a voltage of 35 V_{rms}, meeting the level of requirement for commercial fixed fiber polarizers. However,

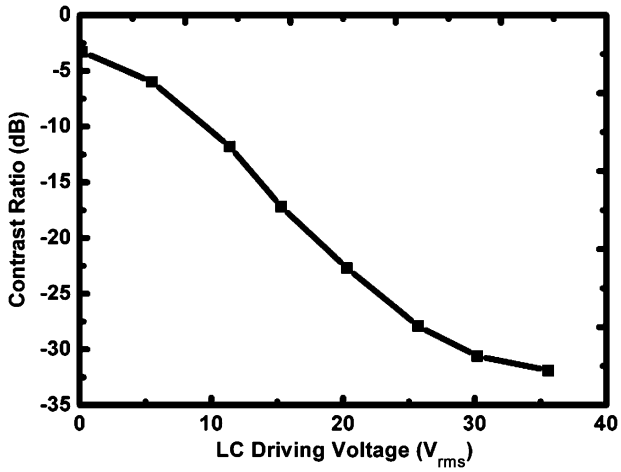

Fig. 4. Voltage-dependent contrast ratio of a LC-based fiber polarizer.

from the figure, the initial extinction ratio is about -3 dB, even though there is no voltage applied. In our opinion, the large LC pretilting angle in the LC cell is responsible for both the light loss and initial extinction ratio without voltage. In other words, the LC molecules are not exactly axially planar-aligned along the fiber at the beginning, which results from the weak anchoring strength on the rubbed fiber. Therefore, the TIR condition is not perfectly fulfilled, bringing about light leak in a way. As our LC cell is kind of special, we have to fabricate it manually. It is hard to control the rubbing process especially on the etched fiber. In addition, the very thick cell gap (125 μm) may also make the LC alignment imperfect and cause light scattering. However, the polarizer's performances at lower driving voltage could be improved by way of adopting a more suitable LC alignment technology, such as photo-alignment [18], and using a thinner cell through multistep etching technique.

Although our LC tunable fiber polarizer is still not ideal, it is already adequate for pressure sensing because of the high polarization contrast. The 393-cm-long fiber between the polarization controller and LC cell is wound to form a coil and placed between two 15 cm $\times$ 15 cm flat glass plates on an optical table. This coil has direct contact with the top and bottom glass plates. Then balance weights with calibrated mass are applied to the top plate gradually, resulting in an increased uniform pressure to the fiber core area. Because the applied forces are transferred to the fiber's axial cross section, whose area is $2lr$ (l is the length of the fiber coil, and r is the fiber radius), the pressure at the fiber core thus could be calculated from the corresponding force and area

$$P = Mg/2lr \tag{1}$$

where P is the pressure applied to the fiber core, and M is the mass of the balance weights applied.

Fig. 5 shows the experimental results of the pressure sensing by using our LC fiber polarizer. A saturated voltage is applied to the LC cell for $\sim$30-dB polarization contrast, which is high enough to obtain a perfect "dark" state with cross polarizers. As we discussed before, the applied pressure results in birefringence in the fiber due to photoelastic effect. There is, thus, phase retardation between the x- and y-polarized lights. At high-contrast-ratio situation, once there is a little change of the polarization state inside the fiber, there would be a detectable variation of the output light intensity. However, when merely a low contrast exists, there would always leaking light which is a noise determining the smallest detectable signal at a low pressure. In our experiment, when there is no pressure applied, almost no output light is detected as it cannot pass a pair of orthogonally placed cross polarizers. When the pressure becomes higher, the output intensity goes up and down, forming a typical sinusoidal curve, as shown in Fig. 5(a). As a consequence, the pressure-induced

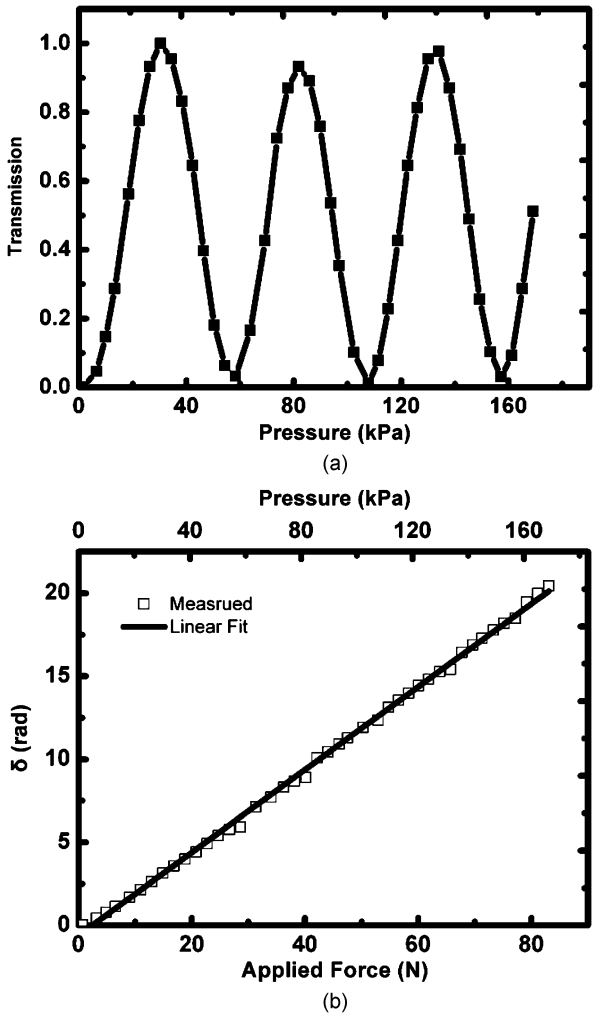

Fig. 5. (a) Pressure-induced transmission change. (b) Measured phase retardation as a function of the applied force. The solid line is a best-fit curve.

phase retardation can be easily deduced from the well-known cross-polarizer interference filter equation

$$\delta = 2 \arcsin I^{1/2} \tag{2}$$

where δ is phase retardation, and I is the light transmittance. The result is shown in Fig. 5(b) with the x-axis title of the applied force F. From the curve, the sensitivity of this pressure sensor is calculated to be $d\delta/dF = 0.25$ rad/N.

Assuming the fiber is fully elastic and mechanically homogeneous, the photoelastic phase retardation induced by the applied force is given by [19]

$$\delta = 8CF/\lambda r \tag{3}$$

where C is the stress-optic coefficient, and λ is the light wavelength. So, a fiber should have the pressure sensitivity of

$$d\delta/dF = 8C/\lambda r. \tag{4}$$

According to Eq. (4), the fiber's stress-optic coefficient, light wavelength, and fiber diameter all play important roles in the sensitivity of such a pressure sensor. Given our measured sensitivity

0.25 rad/N, C is calculated to be 3.03×10^{-12} m^2/N. To our knowledge, there is few report on the stress-optic coefficient measurement of fused silica fiber at 1550-nm telecomm band, but our result is consistent with the tendency of measured values at visible band [20], [21].

The pressure sensing is demonstrated in Fig. 5, while our LC fiber polarizer still has other applications as well. Principally, it may detect any parameter changes associated with light polarization inside a fiber, e.g., environmental magnetic field and electric current in surrounding wires. Furthermore, the LC tunability even gives us more applications that are not convenient for normal fixed polarizers. For example, cascading sensing becomes feasible as our LC polarizer has low IL at voltage-off state. In this situation, a serial of such polarizers could be fabricated on a single long fiber. If we apply saturated voltage to a pair of adjacent polarizers and do not apply voltage to others, any light polarization change between these two polarizers could be detected. However, other zones are just like normal fiber due to their low IL. Then we may activate other two polarizers to detect other zones. Otherwise, if fixed fiber polarizers are used, cascaded fiber sensors may interfere with each other and lead to high propagation loss. Furthermore, if we design a tube-like LC cell to replace the simple planar configuration, whose inside wall is coated with segmented while separate ITO electrodes, one may control the electric field direction around the fiber core. An arbitrarily oriented tunable polarizer is thus obtained. It might have some unique applications in sensitive signal procession, polarization analysis, polarization generation, polarization-mode dispersion (PMD) monitoring, spectrum filtering and control, polarization extinction ratio improvement, fiber laser mode locking, and polarization interferometers.

4. Conclusion

We demonstrated a tunable fiber polarizer and pressure sensor based on LC technology. Its performance is comparable with conventional fixed fiber polarizers. The novel tunability feature further gives rise to many interesting new applications in fiber-optic sensors, measurement equipment, and optical communications.

References

[1] R. L. King, "Information services for smart grids," presented at the General Meeting IEEE Power Eng. Soc., Pittsburgh, PA, 2008.
[2] S. O. Amin, M. S. Siddiqui, C. S. Hong, and S. Lee, "RIDES: Robust intrusion detection system for IP-based ubiquitous sensor networks," *Sensors*, vol. 9, no. 5, pp. 3447–3468, May 2009.
[3] D. K. Yang and S. T. Wu, *Fundamentals of Liquid Crystal Devices*. Chichester, U.K.: Wiley, 2006.
[4] Z. D. Huang, Y. Q. Lu, and S. P. Wang, "Dynamic DWDM channel blocking/equalizing based on liquid crystal technology," *Proc. SPIE*, vol. 7137, pp. 713 71Z-1–713 71Z-8, Oct. 2008.
[5] A. G. Maksimochkin, S. V. Pasechnik, V. A. Tsvetkov, D. A. Yakovlev, G. I. Maksimochkin, and V. G. Chigrinov, "Electrically controlled switching of light beams in the plane of liquid crystal layer," *Opt. Commun.*, vol. 270, no. 2, pp. 273–279, Feb. 2007.
[6] T. J. Chen, J. M. Hsu, and S. H. Chen, "In-line fiber polarization selector and intensity modulator," *Mol. Cryst. Liq. Cryst.*, vol. 304, pp. 415–421, 1997.
[7] X. J. Wang, Z. D. Huang, J. Feng, X. F. Chen, X. Liang, and Y. Q. Lu, "Liquid crystal modulator with ultra-wide dynamic range and adjustable driving voltage," *Opt. Express*, vol. 16, no. 17, pp. 13 168–13 174, Aug. 2008.
[8] T. R. Woliński and W. J. Bock, "Cholesteric liquid crystal sensing of high hydrostatic pressure utilizing optical fibers," *Mol. Cryst. Liq. Cryst.*, vol. 199, pp. 7–17, 1991.
[9] T. R. Woliński, A. Jarmolik, and W. J. Bock, "Development of fiber optic liquid crystal sensor for pressure measurement," *IEEE Trans. Instrum. Meas.*, vol. 48, no. 1, pp. 2–6, Feb. 1999.
[10] T. R. Woliński, A. W. Domanski, W. Konopka, and W. J. Bock, "Prototype fiber optic liquid crystalline sensor for pressure monitoring," *IEEE Trans. Instrum. Meas.*, vol. 48, no. 3, pp. 684–687, Jun. 1999.
[11] D. S. Parmar and H. K. Holmes, "Pressure sensor using liquid crystals," U.S. Patent 5 309 767, May 10, 1994.
[12] W. B. Spillman, "Multimode fiber-optic pressure sensor based on the photoelastic effect," *Opt. Lett.*, vol. 7, no. 8, pp. 388–390, Aug. 1982.
[13] Y. P. Wang, L. M. Xiao, D. N. Wang, and W. Jin, "In-fiber polarizer based on a long-period fiber grating written on photonic crystal fiber," *Opt. Lett.*, vol. 32, no. 9, pp. 1035–1037, May 2007.
[14] K. Zhou, G. Simpson, X. Chen, L. Zhang, and I. Bennion, "High extinction ratio in-fiber polarizers based on 45° tilted fiber Bragg gratings," *Opt. Lett.*, vol. 30, no. 11, pp. 1285–1287, Jun. 2005.
[15] K. Y. Hsu, S. P. Ma, K. F. Chen, S. M. Tseng, and J. I. Chen, "Surface-polariton fiber polarizer: Design and experiment," *Jpn. J. Appl. Phys.*, vol. 36, no. 4B, pp. L488–L490, Apr. 1997.

[16] D. W. Berreman, "Solid surface shape and the alignment of an adjacent nematic liquid crystal," *Phys. Rev. Lett.*, vol. 28, no. 26, pp. 1683–1686, Aug. 1972.
[17] M. Monerie, "Propagation in doubly clad single-mode fibers," *IEEE J. Quantum Electron.*, vol. QE-18, no. 4, pp. 535–542, Apr. 1982.
[18] V. G. Chigrinov, H. S. Kwok, H. Hasebe, H. Takatsu, and H. Takada, "Liquid-crystal photoaligning by azo dyes," *J. Soc. Inf. Display*, vol. 16, no. 9, pp. 897–904, Sep. 2008.
[19] Y. Namihira, M. Kudo, and Y. Mushiake, "Effect of mechanical stress on the transmission characteristics of optical fibers," *Electron. Commun. Jpn.*, vol. 60, pp. 107–115, Jul. 1977.
[20] E. S. Jog and R. S. Krishnan, "Dispersion of the photoelastic constants of fused silica," *Nature*, vol. 179, no. 4558, pp. 540–541, Mar. 1957.
[21] N. K. Sinha, "Normalised dispersion of birefringence of quartz and stress optical coefficient of fused silica and plate glass," *Phys. Chem. Glasses*, vol. 19, no. 4, pp. 69–77, Aug. 1978.